Preparation and Characterization of Core/Shell-like Intumescent Flame Retardant and its Application in Polypropylene

Kun Wu[a]; Lei Song[a]; Zhengzhou Wang[ab]; Yuan Hu[a]; Everson Kandare[c]; Baljinder K. Kandola[c]

[a] State Key Laboratory of Fire Science, University of Science and Technology of China, Anhui, PR China [b] School of Materials Science and Engineering, Tongji University, Shanghai, PR China [c] Center for Materials Research and Innovation, University of Bolton, Deane Road, Bolton, UK

PLEASE SCROLL DOWN FOR ARTICLE

Taylor & Francis
Taylor & Francis Group

Preparation and Characterization of Core/Shell-like Intumescent Flame Retardant and its Application in Polypropylene

KUN WU[1], LEI SONG[1], ZHENGZHOU WANG[1,2,*], YUAN HU[1,*], EVERSON KANDARE[3] and BALJINDER K. KANDOLA[3]

[1] *State Key Laboratory of Fire Science, University of Science and Technology of China, Anhui 230026, PR China*
[2] *School of Materials Science and Engineering, Tongji University, Shanghai 200092, PR China*
[3] *Center for Materials Research and Innovation, University of Bolton, Deane Road, Bolton, BL3 5AB, UK*

With a shell of starch-melamine-formaldehyde (SMF) resin, core/shell-like ammonium polyphosphate (SMFAPP) is prepared by *in situ* polymerization, and is characterized by SEM, FTIR and XPS. The shell leads SMFAPP a high water resistance and flame retardance compared with APP in polypropylene (PP). The flame retardant action of SMFAPP and APP in PP are studied using LOI, UL 94 test and cone calorimeter, and their thermal stability is evaluated by TG. The flame retardancy and water resistance of the PP/SMFAPP composite at the same loading is better than that of the PP/APP composite. UL 94 ratings of PP/SMFAPP can reach V-0 at 30 wt% loading. The flame retardant mechanism of SMFAPP was studied by dynamic FTIR, TG and cone calorimeter, etc.

Keywords: Ammonium polyphosphate, intumescent flame retardation, microencapsulation, PP, thermal degradation

1 Introduction

Polyolefins, such as polyethylene, polypropylene etc., are very important but flammable polymers. In order to reduce their flammability, flame retardants are added. The intumescent flame retardant (IFR) system has aroused great attention in recent years because they are more environmentally friendly than the traditional halogen-containing flame retardant. IFR system is usually composed of three components: an acid source (e.g. ammonium polyphosphate, etc.), a carbonization agent (e.g. pentaerythritol, starch, etc.) and a blowing agent (e.g. melamine, etc.). The classical association of ammonium polyphosphate (APP), pentaerythritol (PER) and melamine (MEL) is an efficient flame retardant (FR) system in polymeric matrices (1). Bourbigot and his co-workers have done extensive studies on the APP intumescent flame retardant system in polyolefins (2–4), and reviewed the recent developments of the IFR systems in great detail (5).

Unfortunately, most IFR systems have some problems such as weak water resistance and poor compatibility with polymer matrix. To deal with the above problems, several methods can be used, such as surface modification with coupling agents (6) and microencapsulation with water-insoluble polymers (7, 8). In our previous work, we coated APP with melamine–formaldehyde (MF) or urea-melamine–formaldehyde (UMF) resin by *in situ* polymerization method (9, 10). Microencapsulated APP (MCAPP) with MF or UMF resin shell decreases its water absorption, and increases its water resistance in PP matrix. Though LOI values of the PP/MCAPP composites increases, it has been found that MCAPP used alone in PP does not pass any rating in the UL 94 test due to the scarcity of carbonization agents. In order to resolve this problem, PER or DPER is used. Though the adding of PER or DPER can increase the flame retardation of PP/MCAPP composites, the existences of PER or DPER may debase the water resistance of PP composites.

Melamine–formaldehyde (MF) resin is commonly used in the microencapsulation, for example red phosphorus (11), *n*-octadecane (12) and phase-change materials (13), etc. Figure 1 shows the reaction scheme of the formation of MF prepolymer and MF resin (14, 15). Starch is an inexpensive and low toxic polysaccharide with many O—H groups and it can be used as a carbonization agent in IFR

*Address correspondence to: Zhengzhou Wang, State Key Laboratory of Fire Science, University of Science and Technology of China, Anhui 230026, PR China and School of Materials Science and Engineering, Tongji University, Shanghai 200092, PR China. E-mail: zwang@ustc.edu.cn; and Yuan Hu, E-mail: yuanhu@ustc.edu.cn
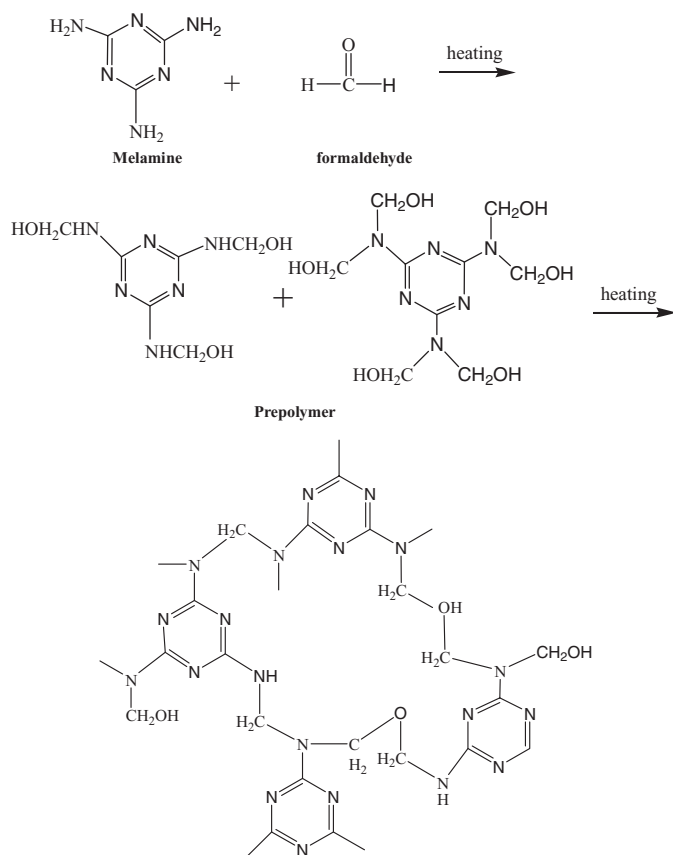
Fig. 1. The reaction scheme of the formation of MF prepolymer and MF resin.

2 Experimental

2.1 Materials

APP with an average degree of polymerization n > 1000 was kindly supplied by Hangzhou JLS Flame Retardants Chemical Corporation. Starch, melamine and formaldehyde were purchased from the Shanghai Chemical Reagent Corporation. PP (F401) with a melt flow index (MFI) of 2.3 g/10 min^{-1} (230°C/2.16 kg) was provided by Yangzi Petroleum Chemical Company.

2.2 Preparation of Core/Shell-like APP

Synthesis of prepolymer: Starch (6, 9, 12, 15 or 18 g), 4 g melamine and 100 ml distilled water were put into a three-neck bottle with a stir. The mixture was adjusted to pH 4–5 with acetum, heated to about 90°C and kept at that temperature for 1.5 h. After that, the pH was adjusted by 10% Na_2CO_3 solution to 8–9, 4 g melamine and 10 ml 37% formaldehyde solution were added into the system. The temperate was kept at 90°C for 1 h. The prepolymer solution was prepared and ready for the next step.

Preparation of core/shell-like APP: 40 g APP was first dispersed in 100 ml ethanol with a stir (1000 rpm, 5 min). The prepolymer solution obtained from the above step was added into the mixture, and the pH of the mixture was adjusted to 4–5 with sulfuric acid. The resulting mixture was heated at 80°C for 2 h. After that, the mixture was cooled to room temperature, filtered, washed with distilled water, and dried at 105°C, and the SMFAPP powder was finally obtained. The theoretical principal polymer repeat unit for shell of SMFAPP microcapsules is shown in Figure 2.

2.3 Preparation of Flame Retarded PP Composites

All flame retarded PP composites were prepared in a Brabender-like apparatus at a temperature about 180°C for 15 min. After mixing, the samples were hot-pressed at about 180°C under 10 MPa for 10 mins into sheets of a suitable thickness for analysis.

2.4 Measurements

2.4.1. *Fourier transform infrared spectra*

Powders were mixed with KBr powders, and the mixture was pressed into a tablet. The Fourier transform infrared (FTIR) spectra of samples were recorded using a Nicolet MAGNA-IR 750 spectrophotometer.

Real time FTIR spectra were recorded using the above spectrophotometer equipped with a ventilated oven having a heating device. The temperature of the oven was raised at a heating rate of about 10°C/min. Dynamic FTIR spectra were obtained *in situ* during the thermal degradation of the samples.

system. As a result, we synthesize prepolymer containing starch modified MF and then use the prepolymer to microencapsulate APP. Our aim is to obtain core/shell-like intumescent flame retardant which contains three components of a typical IFR system: APP (as an acid source), starch (as a carbonization agent) and melamine (as a blowing agent). The advantage is to synthesize a flame retardant which may have better water resistance and flame retardance in polymer than an APP IFR system.

In this paper, core/shell-like ammonium polyphosphate (SMFAPP) with a starch-melamine-formaldehyde (SMF) resin shell was prepared by *in situ* polymerization and characterized by water solubility, Fourier transform infrared (FTIR), thermogravimetry (TG) and X-ray photoelectron spectroscopy (XPS), etc. The use of SMFAPP as a flame retardant in PP is evaluated by limiting oxygen index (LOI), UL-94, TG, cone calorimeter and scanning electron microscopy (SEM), and the results from SMFAPP and APP are compared. The flame retardant mechanism of SMFAPP was studied by dynamic FTIR. Moreover, the water resistance of the PP composites containing SMFAPP (or APP) is studied by a decrease of LOI value and water leaching rate.
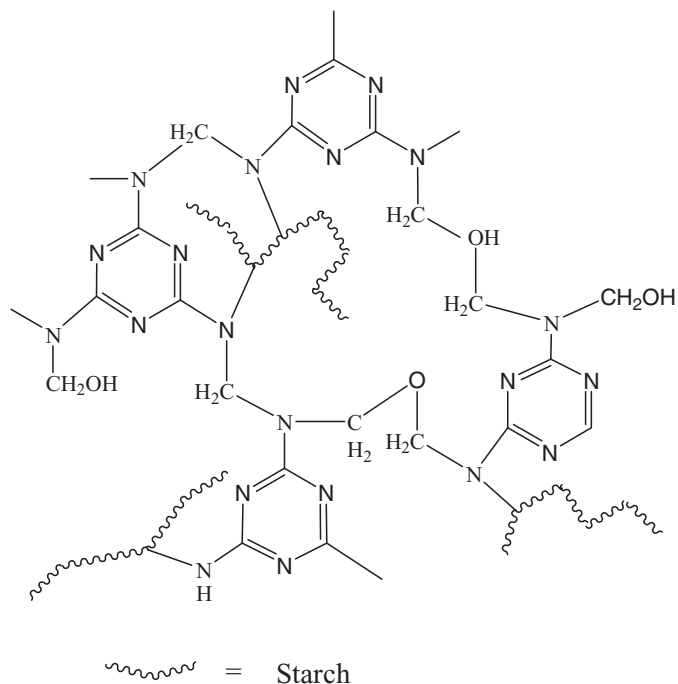
Fig. 2. Supposed principal polymer repeat unit for shell of microcapsules.

2.5 X-ray Photoelectron Spectroscopy Spectra

The X-ray photoelectron spectroscopy (XPS) spectra were recorded with a VG ESCALAB MK II spectrometer using Al kα excitation radiation (hν = 1253.6 eV).

2.6 Granulometry

The particle size distribution was determined by a laser diffraction particle analyzer (RISE2006, Jinan Rise science Co. Ltd, China). Before the measurement, the samples were dispersed in ethanol, and sonicated for 5 minutes.

2.7 Solubility in Water

Sample (about 10 g) was put into 100 ml distilled water at a different temperature and stirred at that temperature for 60 min. The suspension was then filtered. 50 ml of the filtrate was taken out and dried to a constant weight at 105°C. Solubility of samples in water can be calculated.

2.8 Scanning Electron Microscopy

The SEM micrographs of the particles and PP composites were obtained with a scanning electron microscope AM-RAY1000B. The particles were sprinkled onto a double-sided tape, sputter coated with gold layer. The composites were cryogenically fractured in liquid nitrogen, and then sputter coated with the conductive layer.

2.9 Content of the SMF Resin Measurement

Few APP or SMFAPP powder was dissolved in nitric acid at 150°C, and inductively coupled plasma atomic emission spectrometry (Atomscan Advantage, Thermo Jarrell Ash Corporation, USA) was used to measure the phosphorus content of APP or SMFAPP. The symbols $P_{SMFAPP}\%$ and $P_{APP}\%$ represent the percentage of phosphorus in SMFAPP and APP, respectively.

Assuming the content of phosphorus remains constant in the process of the microencapsulation of APP, there the following equation exists:

$$M_{APP} \times P_{APP}\% = M_{SMFAPP} \times P_{SMFAPP}\%$$

Where M_{APP} is the content of APP used, and M_{SMFAPP} is the content of SMFAPP obtained. Therefore, the percentage of the SMF resin (W_{resin} wt%) in SMFAPP can be expressed as follows:

$$W_{resin} \text{ wt}\% = 1 - M_{APP}/M_{SMFAPP}$$
$$= (1 - P_{SMFAPP}\%/P_{APP}\%) \times 100\%$$

If $P_{SMFAPP}\%$ and $P_{APP}\%$ are measured, W_{resin} wt% can be calculated.

2.10 Limiting Oxygen Index

LOI was measured according to ASTM D2863. The apparatus used was an HC-2 oxygen index meter (Jiangning Analysis Instrument Company, China). The specimens used for the test were of dimensions 100 × 6.5 × 3 mm.

2.11 UL- 94 Testing

The vertical test was carried out on a CFZ-2-type instrument (Jiangning Analysis Instrument Company, China) according to the UL 94 test standard. The specimens used were of dimensions 130 × 13 × 3 mm.

2.12 Water Leaching Rate

The specimens (marked Wa) used for measurement were put in distilled water at 50°C and w kept at this temperature for 24 h. The treated specimens were subsequently taken out, and dried to constant at 105°C (marked Wc). The water leaching rate of the specimens can be expressed as (Wa–Wc)/Wa × 100%.

2.13 Thermogravimetry (TG)

Each sample was examined under air flow on a DTG-60H apparatus (Shimadzu Company) at a heating rate of 10°C/min.

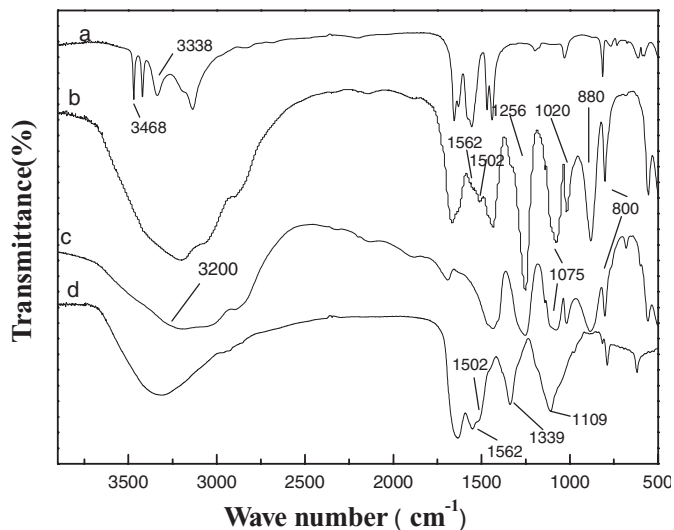**Fig. 3.** FTIR spectra of (a) melamine; (b) SMFAPP; (c) APP; (d) SMF resin.

Fig. 4. XPS spectra of APP and SMFAPP.

2.14 Cone Calorimeter

The combustion tests were performed on the cone calorimeter (Stanton Redcroft, UK) tests according to ISO 5660 standard procedures, with $100 \times 100 \times 3$ specimens. Each specimen was wrapped in aluminium foil and exposed horizontally to 35 kW/m^2 external heat flux.

3 Results and Discussion

3.1 FTIR and XPS

The FTIR spectra of melamine, SMFAPP, APP and SMF resin are shown in Figure 3. For melamine, the NH$_2$ group gives rise to absorption at 3550–3330 cm^{-1} (asymmetric stretch) and at 3450–3250 cm^{-1} (symmetric stretch) (16). The above peaks disappear in SMF resin; it may be caused by the reactions between melamine and starch/formaldehyde. Bands in the region from 3250 to 3500 may be due to the OH of starch or NH stretching vibrations of MF resin (16). The band at 1109 cm^{-1} can be assigned the C–O stretching of the ring of the starch (17). The absorptions of 1562, 1502 and 1339 cm^{-1} are due to the ring vibration of melamine group from the SMF resin (11). It is clear that for SMFAPP, the main absorption peaks appear at 3200, 1562, 1502, 1256, 1075, 1020, 880 and 800 cm^{-1}. The typical absorption peaks of APP include 3200 (N-H), 1256 (P=O), 1075 (P–O symmetric stretching vibration), 880 (P–O asymmetric stretching vibration), 1020 (symmetric vibration of PO$_2$ and PO$_3$), and 800 (P–O–P) cm^{-1}(18). The spectrum of SMFAPP reveals not only well-defined absorption peaks of SMF resin, but also the characteristic bands of APP, indicating that the resin exist in the SMFAPP.
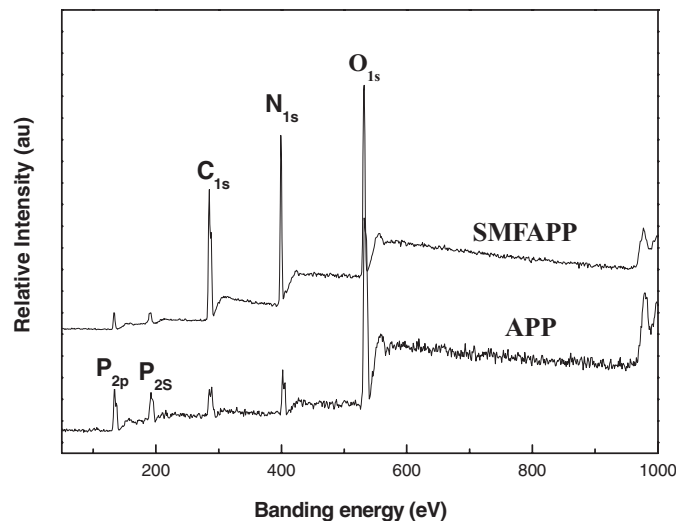
Figure 4 shows XPS spectra of APP and SMFAPP. It can be seen that the peaks located at 134.7 and 190.9 eV are attributed to P$_{2P}$ and P$_{2S}$ of APP. For SMFAPP, the intensities of peaks aforementioned decrease sharply, meanwhile the intensities of the C$_{1S}$ and N$_{1S}$ peaks centered at 284.7 and 397.9 eV, respectively increase greatly. The changes of the above peaks are due to the coverage of the outside APP particles with the starch-melamine-formaldehyde resin, which indicates that APP was well coated by the resin.

3.2 Size Distribution and Morphology

The particle size distributions of APP and SMFAPP are shown in Figure 5. It can be found that the size distribution of APP is wider than that of SMFAPP. Due to the microencapsulation, the D50 value of MUFAPP is 13.577 μm, smaller than APP's 20.296 μm. This can be explained by the fact that APP particles are easily attacked by moisture and tend to agglomerate. From the difference of size distribution, it is expected that SMFAPP would have better dispersion in polyolefins than APP when SMFAPP is blended with the polymers.

Figure 6 shows the surface morphologies of APP and SMFAPP. It is clear that the surface of APP particle is very smooth, as Figure 6a shows. After microencapsulation, SMFAPP presents a comparably rough surface. It is also interesting to find that some smaller particles with a diameter less than 0.1 μm are scattered on the surface of SMFAPP, and they appear to be SMF resin microparticles.

The above results also suggest a coating of APP with the SMF resin.

3.3 Water Solubility of SMFAPP

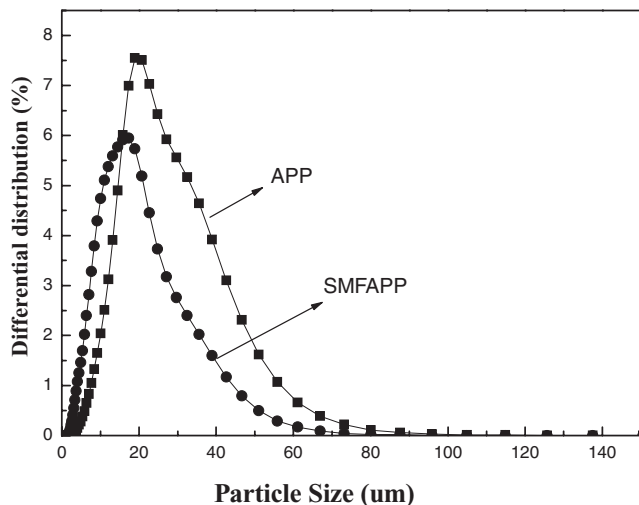Figure 7 shows the influence of content of starch in prepolymer on the water solubility of SMFAPP. From Figure 7, it

Fig. 5. Particle size distributions of APP and SMFAPP.

Fig. 7. Solubility of APP and SMFAPP versus content of starch in prepolymer.

can be seen that the solubility of APP without microencapsulation at 25°C and 80°C is 0.47 and 2.4 g/100 ml H_2O, respectively, indicating that APP can be easily attacked by moisture or water, especially at high temperatures. After the microencapsulation of APP with SMF resin, the solubility of SMFAPP decreases above 90% at 25°C. As the content of the starch increases further, the solubility of SMFAPP changes little. The change trend of solubility of SMFAPP at 80°C is similar to that of SMFAPP at 25°C. It is interesting to find that there is a great difference of solubility of APP at 25°C and 80°C. However, the difference of solubility of SMFAPP at 20°C (0.02 g/100 ml H_2O) and 80°C
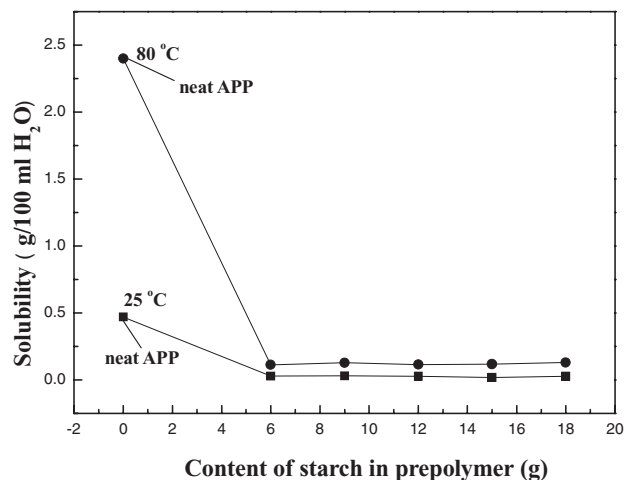
(0.12 g/100 ml H_2O) is small. This is because the SMF resin outside APP is hydrophobic, leading to the decrease of the solubility of APP. The above results also indicate that APP was well microencapsulated by the resin.

3.4 Flame Retardation of PP Composites

The influence of starch content in prepolymer on the LOI values of PP/SMFAPP composites is shown in Figure 8. SMFAPP is the blend with PP at the mass percentage of 30%. From the figure, it can be seen that with the increase of starch content, LOI value increase. It is suggested that
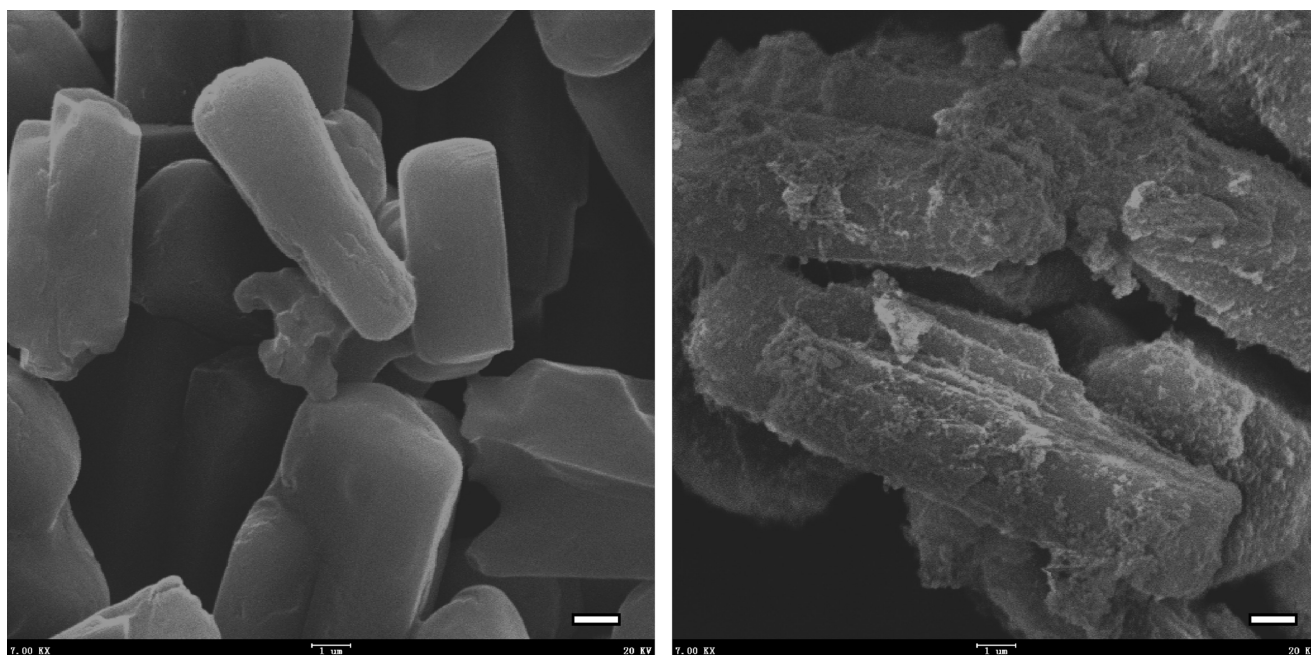

Fig. 6. SEM micrographs of surface morphology ($\times$ 7000): (a) APP and (b) SMFAPP; Scale-bars represent 1 μm.
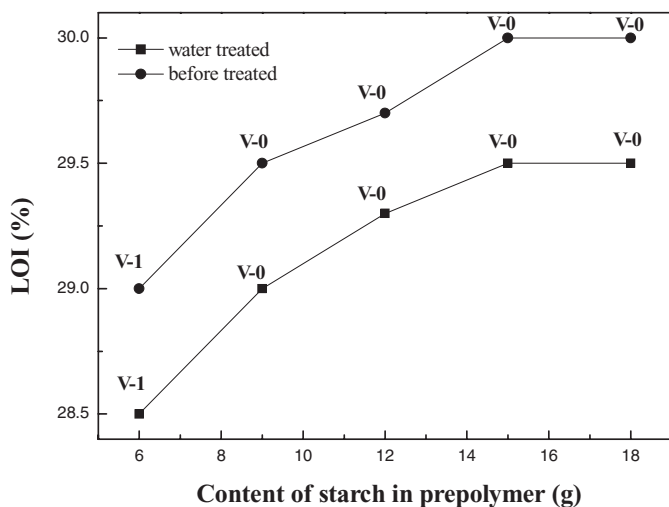
Fig. 8. LOI values of PP/SMFAPP before and after water treatment vs. content of starch in prepolymer.

Fig. 9. Water leaching rate of PP/APP and PP/SMFAPP vs. content of starch in prepolymer.

a suitable phosphorus/nitrogen/carbon ratio in the IFR system is very important for the flame retardation of FR composites. Also, it should be noticed that the UL 94 results of most of PP/SMFAPP composites can reach V-0. From the above results, the SMFAPP sample prepared with pre-polymer containing 15 g starch was selected for the flame retardation of PP composites. And from the equation of 2.5.5, it can be calculated that this SMFAPP sample is coated with 24.8% resin.

The LOI value of the composite containing 30% SM-FAPP (coated with 24.8% resin) is 30.0%, while the value of the PP/APP or PP/APP/PER (mass ratio of APP and PER is 1:1) composite at the same additive level is only 20.0% and 28.0% (9). It is clear that APP used alone in PP does not have good flame retardancy (no ratings in the UL-94 test), the reason for this is due to the scarcity of car-bonization and blowing agent. When PER is incorporated into the PP/APP composites, a remarkable improvement of flame retardation is observed. But it should be noticed that due to the presence of SMF resin outside APP, the LOI value of PP/SMFAPP is higher than that of PP/APP/PER composites. The explanation for the increase may be due to the fact that when the PP composites containing SM-FAPP are heated, the resin in the coating layer of APP releases water vapor and NH_3 gases which would reduce the concentration of air and make the material swell to form intumescent char.

3.5 Water Resistance of FR PP Composites

Water leaching rates of PP/APP and PP/SMFAPP vs. content of starch in prepolymer are shown in Figure 9. It can be seen that through microencapsulation, the leaching rate of FR PP composites reduces greatly, from 9.81% to 0.23% as the percentage of SMFAPP in PP composites is 30%. It
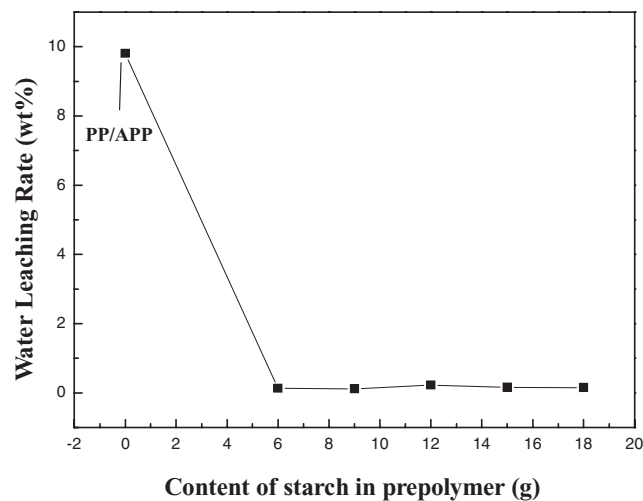
also can be found that due to the hydrophobicity of SMF resin, with the increase of content of starch in prepolymer, leaching rates of PP/SMFAPP change little. So when expo-sure in water medium, the comparatively better dispersion and less solubility of SMFAPP in PP matrix would prevent IFRs from being exuded, and a certain flame retardancy of composite can still be maintained.

The changes of flame retardation of the PP composites containing APP or SMFAPP after the hot water treatment (50°C, 24 h) are shown in Figure 8. For the PP/APP bi-nary composite at 30.0% additive level, their LOI values are about 20.0% before the treatment, and the values de-crease by 2.5% after the hot water treatment. The LOI value of some of PP/SMFAPP composite at a loading 30% are 30.0%, whereas the value is still as high as 29.5% after the treatment. In spite of the decrease in the LOI values of the PP/SMFAPP composites after treated, a good main-taining the UL-94 ratings is observed (most are still V-0 rat-ing). Moreover, though PP/APP/PER or PP/APP/DPER composites can reach V-1 in UL 94 testing, there were no ratings for above ternary composites after water treatment (50°C, 24 h) (9, 10). Therefore, the conclusion can be drawn that the water resistance of SMFAPP is much better than the APP intumescent flame retardant system in PP com-posites.

The fractured surface of PP/APP and PP/SMFAPP composites before and after water treatment was observed by SEM, shown in Figure 10 (a), (b), (c) and (d). Before water treated, APP grains are distributed unevenly in PP matrix and an abundance of grains are exposed on the sur-face, a clear interfacial line can be observed at the interface. So when the composites are exposed to water medium, the water molecules will absorb on the surface of the material, and some APP grains on the surface would dissolve in the water, leaving some defects on the surface. In comparison with APP, it can be seen that in Figure 10 (c) nearly all of
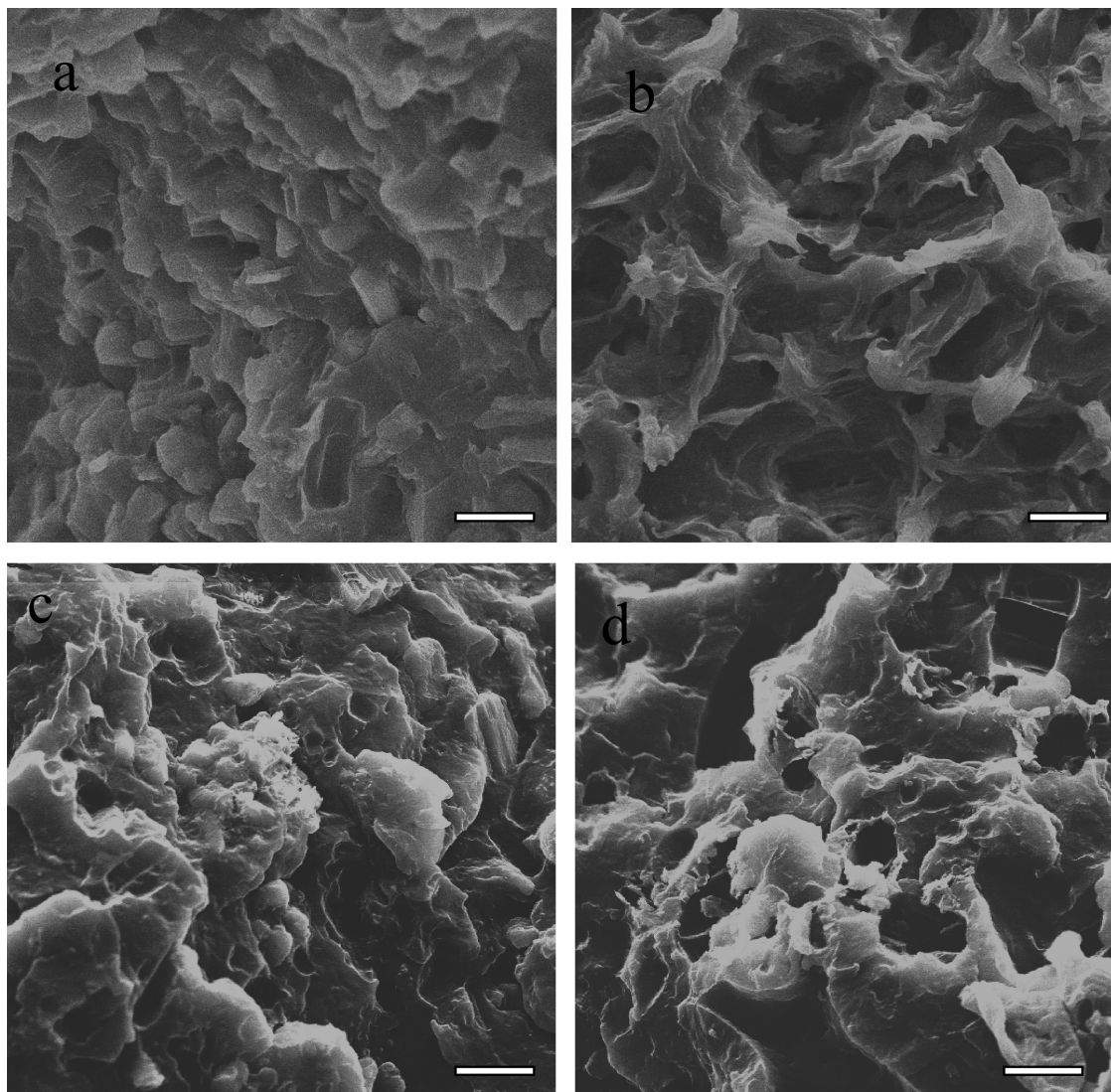
Fig. 10. SEM micrographs of fracture surfaces of the composites ($\times$ 1500): (a) PP/APP; (b) PP/APP (50°C, 24 h); (c) PP/SMFAPP; (d) PP/SMFAPP (50°C, 24 h). Scale-bars represent 10 μm.

SMFAPP particles are in the matrix, and such structure is good for the water resistance of FR composites. So, after treated at 50°C for 24 h, there are still some grains left in PP matrix. The above results indicate that core/shell structure have a remarkable effect on the water resistance of APP in PP matrix.

3.6 Thermal Analysis

The TG and DTG curves of APP and SMFAPP are shown in Figure 11. APP has two main decomposition processes. It begins to decompose at about 270°C. The evolution products in the first process are mainly ammonia and water (about 20% mass loss), and crosslinked polyphosphoric acids (PPA) are formed simultaneously (19). The second process occurs in the range 500–700°C, which is the main decomposition process of APP, and weight loss is about 78%. The temperatures of maximum mass loss rate (T_{max}) for the two steps are 326°C and 625°C, respectively, as shown in Figure 11B. The residual weight of APP is 0.6% at 800°C.

It can be seen that the initial decomposition temperature of SMFAPP is similar with that of APP. However, at the lower temperature, SMFAPP decomposes faster than APP owing to the less thermal stability of SMF resin in SMFAPP and the esterification between APP and starch. The resin outside APP on heating produces nonflammable gases, such as NH_3 and CO_2, which are helpful in forming a "honeycomb" char structure. So beyond the temperature of 599°C, SMFAPP is more stable than APP. The T_{max} values for main two steps of SMFAPP decomposition are 392 and 584°C, respectively. Moreover, SMFAPP after decomposition at 800°C left about 28.4% residue, which is much higher than that of APP.
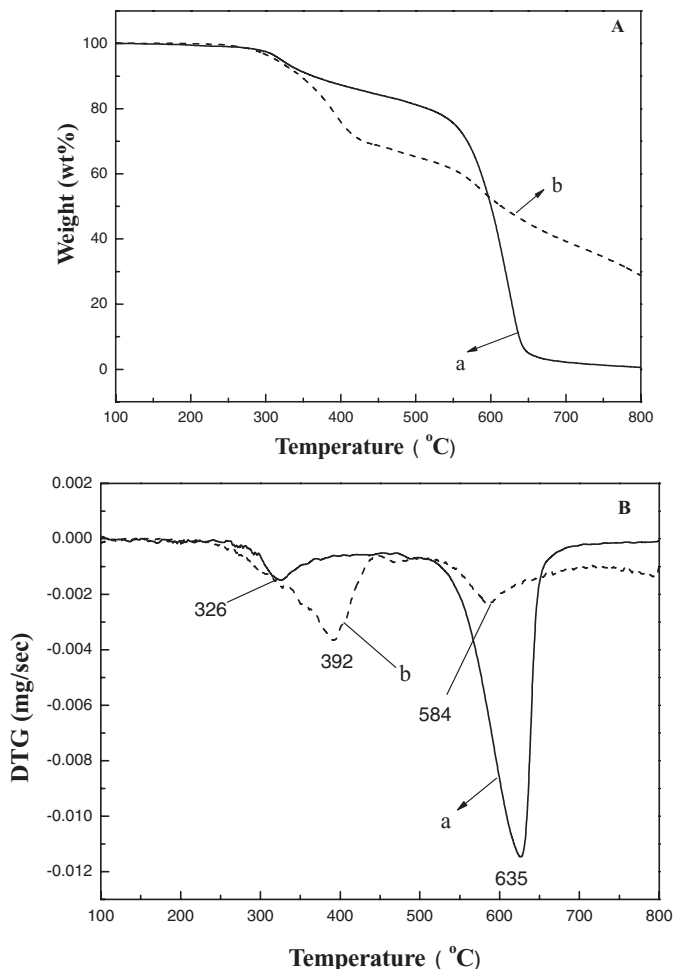
Fig. 11. TG (A) and DTG (B) curves of (a) APP and (b) SMAFPP.

Fig. 12. TG (A) and DTG (B) curves of (a) PP; (b) PP/APP; (c) PP/SMFAPP.

The TG and DTG curves of PP and the PP composites containing 30 wt% flame retardant are shown in Figure 12. It is clearly seen that the pure PP begins to decompose at about 240°C and almost decomposes completely at 360°C. The T_{max} of the decomposition is 299°C, as shown in Figure 12 A.

The thermal decomposition of the PP/APP composite includes three steps. Its initial decomposition temperature is a bit higher than that of PP. The composite PP/APP decomposes initially at about 250°C, which is caused by the decomposition of APP. The second step of mass loss is the main decomposition process of PP in the composite, and its T_{max} in this step is 366°C. The third step occurs at above 500°C due to the further decomposition of the char.

It can be seen in Figure 12A that the decomposition of PP/SMFAPP is similar with PP/APP at lower temperature. However, at the temperature higher than 360°C, the composite containing with SMFAPP is more thermally stable than the composite containing APP. The T_{max} values of the main decomposition steps of PP/SMFAPP are 276, 349 and 632°C, respectively. The residue left at 800°C of PP/SMFAPP is 1.7% which is high than that of PP/APP.
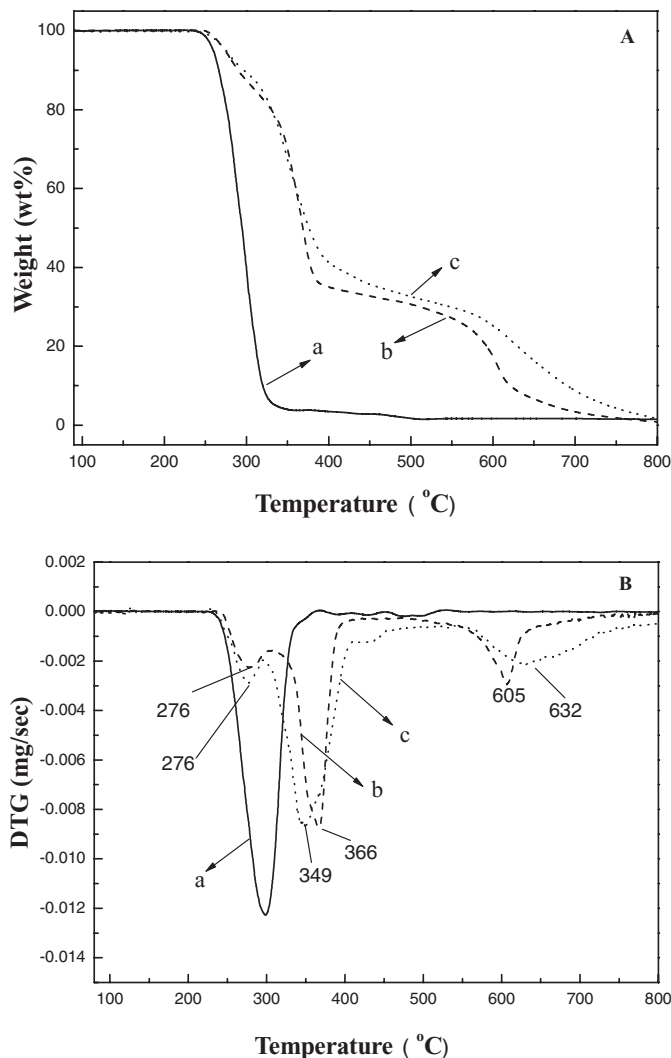
The increase of amount of residue of the composite may be due to the formation of more thermally stable char. From the above results, the conclusion can be drawn that SM-FAPP is better than APP in improving the thermal stability of the PP composite at high temperature.

3.7 Thermal Degradation of SMFAPP

To study the flame retardant mechanism of SMFAPP in polymers, we used dynamic FTIR to evaluate the thermal degradation of SMFAPP.

For SMFAPP (Figure 13), no modification of the chemical structure is observed below 250°C. With the increase of temperature, above 250°C, the bands which correspond to -NH_4 (1434 cm^{-1}) of APP (16) disappear; this may be related with the elimination of NH_3. These results demonstrate that the evolution products in the first process are mainly ammonia and water, and crosslinked polyphosphoric acids
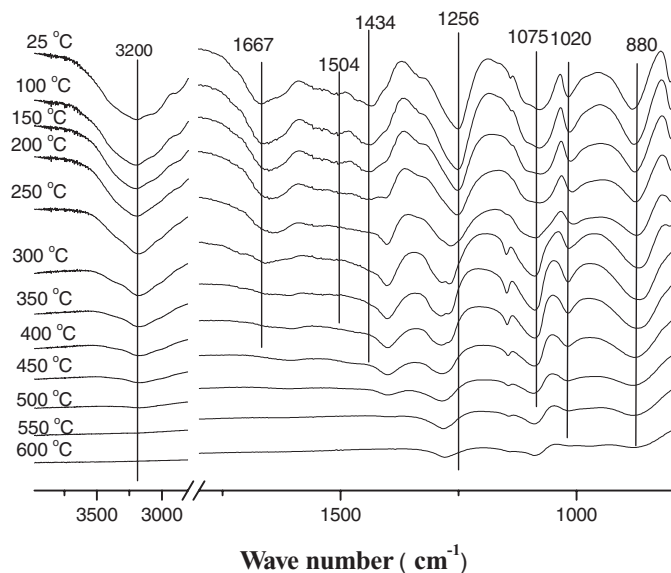
Fig. 13. Dynamic FTIR spectra of SMFAPP with different pyrolysis temperatures.

Fig. 14. Heat release rate curves of PP, PP/APP and PP/SMFAPP.

(PPA) are formed simultaneously. As the pyrolysis temperature increases, the 1256 cm^{-1} peak (P=O) move to a higher waver number (18). It may be caused by the scission of P-O-N of APP and dehydration of PPA and starch. Moreover, we should notice the absence of the absorptions of 1560 cm^{-1} which are due to the ring vibration of melamine groups (11) at about 350°C; it can be explained by the fact that melamine is disassociated and evaporates at higher temperatures. It is interesting to find that between the range of 400 and 600°C, the shape of spectra show few changes. It may be related with the formation of stable structures containing P—O—P and P=O (1075, 1020, 880 cm^{-1}) complexes (11).

These dynamic thermal degradation data give positive evidence of the flame retardant mechanism: SMFAPP can release the acid and form a stable charred layer in the condensed phase during burning of polymer materials, and the shell outside SMFAPP releases water vapor and NH$_3$ gases which would reduce the concentration of air and make the material swell to form intumescent char. These char slow down heat and mass transfer between the gas and condensed phases and prevent the underlying polymeric from further combust. These results are in agreement with the data of TG, LOI and UL 94.

3.8 Cone Calorimeter Study

Cone calorimetry is an effective approach to evaluate the combustion behavior of flame retarded polymers. Heat Release Rate (HRR) results of PP and FR PP composites containing 30 wt% flame retardant are shown in Figure 14. The presence of IFR systems in PP decreases the HRR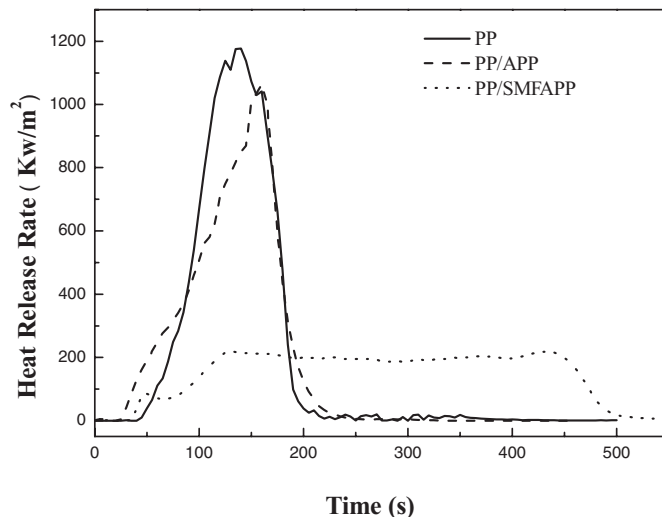 values strongly compared with pure PP (the HRR peak of pure PP is 1177 kW/m^2). In the case of the PP/APP composite, its HRR peak is behind that of pure PP, and its value is a little lower (1064 kW/m^2) than that of PP. However, it is noted that the ignition time (IT) of the PP/APP composite (24 s) is smaller than that of PP (44 s). The reason may be due to the fact that APP decomposes earlier than pure PP after the cone heater irradiated the surface of the composite, and some small volatile molecules are produced from the decomposition of APP.

It can be see in Figure 14 that the HRR curve of PP/SMFAPP is very flat and the values of HRR decrease sharply compared with PP/APP or PP. It is noteworthy that the HRR curve of the PP/SMFAPP is a typical one of IFR systems. Its HRR curve exhibits two peaks. The first peak is assigned to the ignition and to the formation of an expanded protective shield. The second peak is explained by the destruction of the intumescent structure and the formation of a carbonaceous residue (5). Associated data for the PP/SMFAPP are: IT = 37 s, PkHRR = 219 kW/m^2. The addition of SMFAPP in PP leads to a delay in the time to ignition and strongly prolongs the process of combustion compared with PP/APP composite. From this data, it can be concluded that the microencapsualtion can enhance the flame retardant properties of PP/APP system remarkably.

The appearance of FR PP composites residues at the end of cone calorimeter tests were shown in Figure 15. It is clear that there is almost no residue left at the end of the cone calorimeter test for PP/APP composite. On the other hand, the surface of PP/SMFAPP residue is covered with an expanded char network. The residue left by PP/SMFAPP is mainly formed of thick black char which is better than that of PPAPP when protect the underlying materials. It can be concluded that a good and coherent char can prevent the heat transfer and flame spread, and thus protect the underlying materials from further burning.
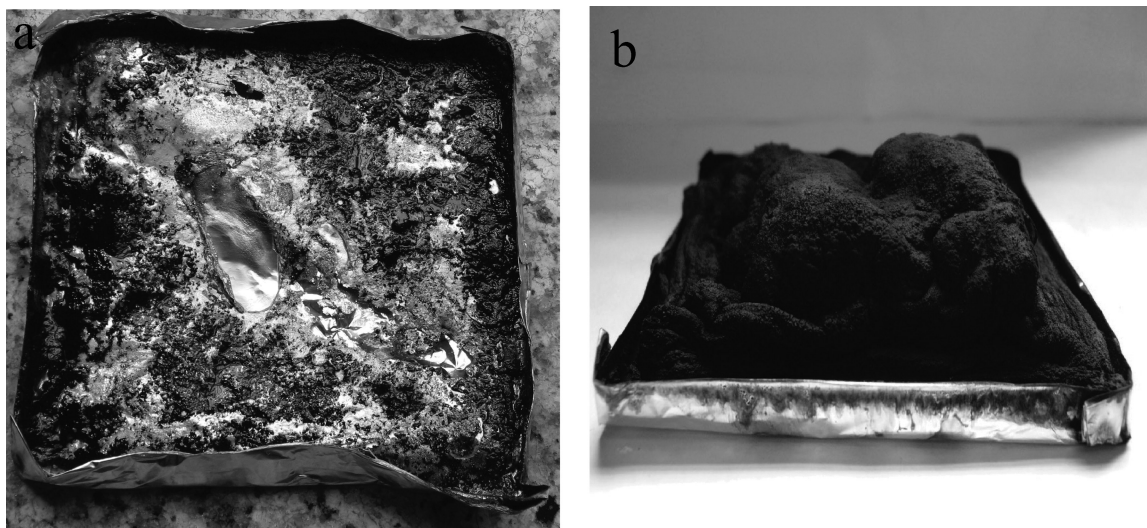
Fig. 15. Residues at the end of cone calorimeter test: (a) PP/APP; (b) PP/SMFAPP.

4 Conclusions

In this work, APP was microencapsulated with starch-melamine-formaldehyde resin by an *in situ* polymerization method to obtain core/shell-like IFR. Core/shell-like APP (SMFAPP) decreases its water solution, increases its water resistance and flame retardance in PP. The LOI values of the PP/SMFAPP composites increases compared with that of the PP/APP or PP/APP/PER composites at the same loading. It has been found that APP used alone in PP does not reach UL-94 V-0 rating and SMFAPP used alone in PP can reach V-0 at the additive level 30%. It also can be found that after water treatment at 50°C for 24 h, the PP/SMFAPP could still maintain good flame retardant properties (V-0).

The flame retardant mechanism of SMFAPP is evaluated by dynamic FTIR, TG and cone calorimeter, etc. Owing to the existence of the shell, SMFAPP can form a stable charred layer in the condensed phase during the combustion of FR composites, release water vapor and NH_3 gases which would reduce the concentration of air and make the material swell to form intumescent char. The intumescent and stable char may prevent the underlying materials from further burning.

Acknowledgements

References

1. Liu, M.F., Liu, Y. and Wang, Q. (2007) *Macromol. Mater. Eng.*, 292, 206–213.
2. Le Bras, M., Bourbigot, S., Delporate, C., Siat, C. and Le Tallec, Y. (1996) *Fire Mater.*, 20, 191–203.
3. Almeras, X., Le Bras, M., Hornsby, P., Bourbigot, S., Marosi, G., Keszei, S. and Poutch, F. (2003) *Polym. Degrad. Stab.*, 82, 325–331.
4. Almeras, X., Le Bras, M., Poutch, F., Bourbigot, S., Marosi, G. and Anna, P. (2003) *Macromol. Symp.*, 198: 435–447.
5. Bourbigot, S., Le Bras, M., Duquesne, S. and Rochery, M. (2004) *Macromol. Mater. Eng.*, 289, 499–511.
6. Metin, D. and Tihminlioglu, F. (2004) *Compos. Part A: Appl. Sci. Manufactur.*, 35, 23–32.
7. Saihi, D., Vroman, I., Giraud, S. and Bourbigot, S. (2005) *React. Funct. Polym.*, 64, 127–138.
8. Saihi, D., Vroman, I., Giraud, S. and Bourbigot, S. (2006) *React. Funct. Polym.*, 66, 1118–1125.
9. Wu, K., Wang, Z.Z. and Liang, H.J. (2008) *Polym. Compos.*, 29, 854–860.
10. Wu, K., Wang, Z.Z. and Hu, Y. (2008) *Polym. Adv. Technol.*, 19, 1118–1125.
11. Wu, Q., Lv, J.P. and Qu, B.J. (2003) *Polym. Int.*, 52, 1326–1331.
12. Zhang, X.X., Fan, Y.F., Tao, X.M. and Yick, K.L. (2004) *Mater. Chem. Phys.*, 88, 300–307.
13. Shin, Y., Yoo, D. and Son, K. (2005) *J. Appl. Polym. Sci.*, 96, 2005–2010.
14. Yuan, L., Liang, G.Z., Xie, J.Q., Li, L. and Guo, J. (2006) Polymer, 47, 5338–5349.
15. Lee, Y.H., Kim, C.A., Jang, W.H., Choi, H.J. and Jhon, M.S. (2001) *Polymer*, 42, 8277–8283.
16. Colthup, N.B., Daly, L.H. and Wiberley, S.E. Introduction to Infrared and Raman Spectroscopy, 2nd ED, Academic Press: Boston, 1990.
17. Rubens, P., Snauwaert, J., Heremans, K. and Stute, R. (1999) *Carbohydr. Polym.*, 39, 231–235.
18. Bugajny, M., Bourbigot, S. and Le Bras, M. (1999) *Polym. Int.*, 48, 264–270.
19. Camino, G., Grassie, N. and McNeill, I.C. (1978) *J. Polym. Sci., Polym. Chem. Ed.*, 16, 95–106.